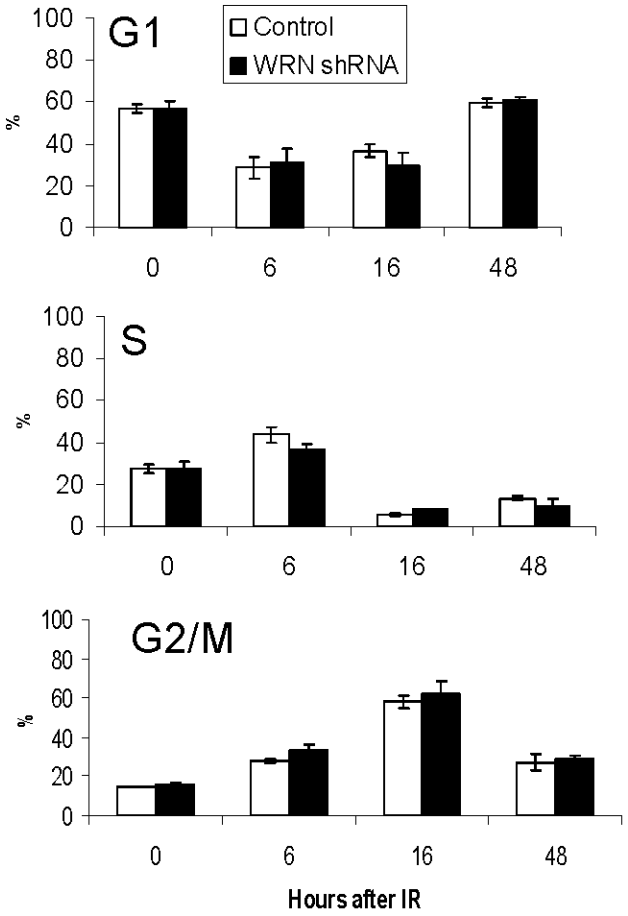

Quantification of cell cycle profiles shown in Fig. 1d. Control and WRN shRNA cells are collected 0, 6, 16, Or 48 h after cellular exposure to 6 Gy γ-irradiation for flow cytometric analysis.

Cheng et al. Supplemental Fig S1

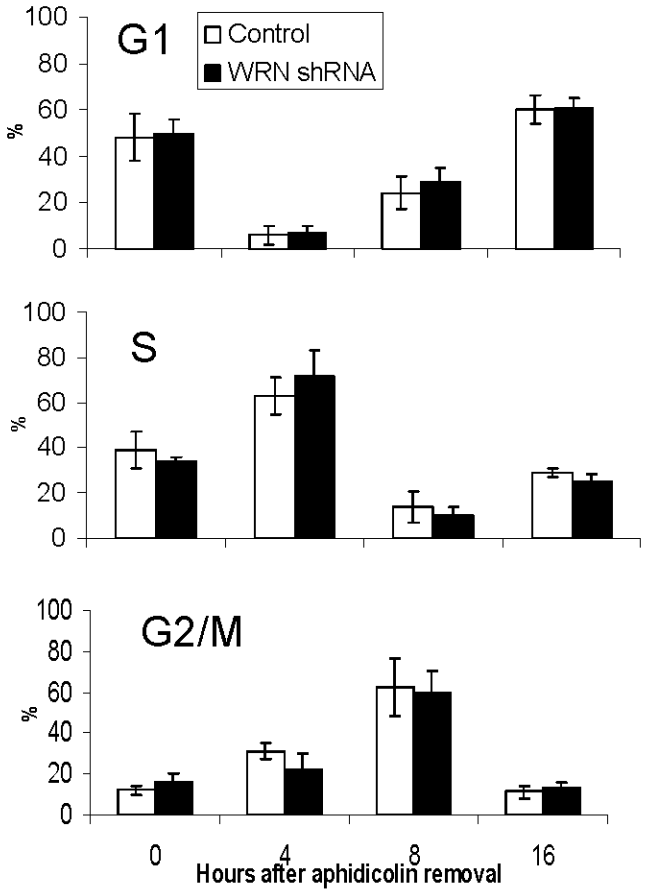

Quantification of cell cycle profiles shown in Fig. 1e. Control and WRN shRNA cells are collected 0, 4, 8, Or 16 h after aphidicolin removal (1 μg/ml for 24 h) for flow cytometric analysis.

Cheng et al. Supplemental Fig S2

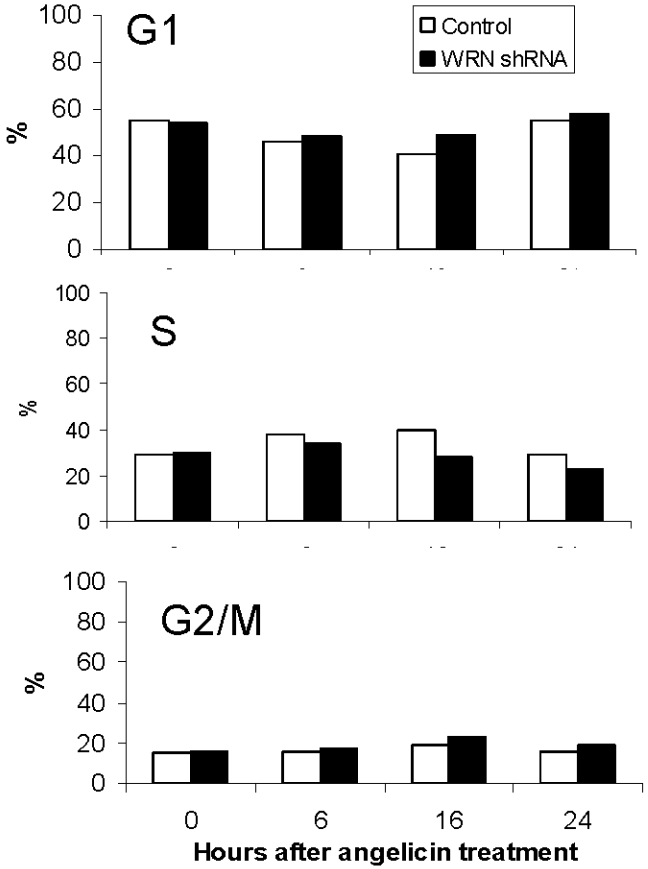

Quantification of cell cycle profiles shown in Fig. 1a. Control and WRN shRNA cells are collected 0, 6, 16, or 24 h after angelicin treatment (0.1 μg/ml) for flow cytometric analysis.

Cheng et al. Supplemental Fig S3

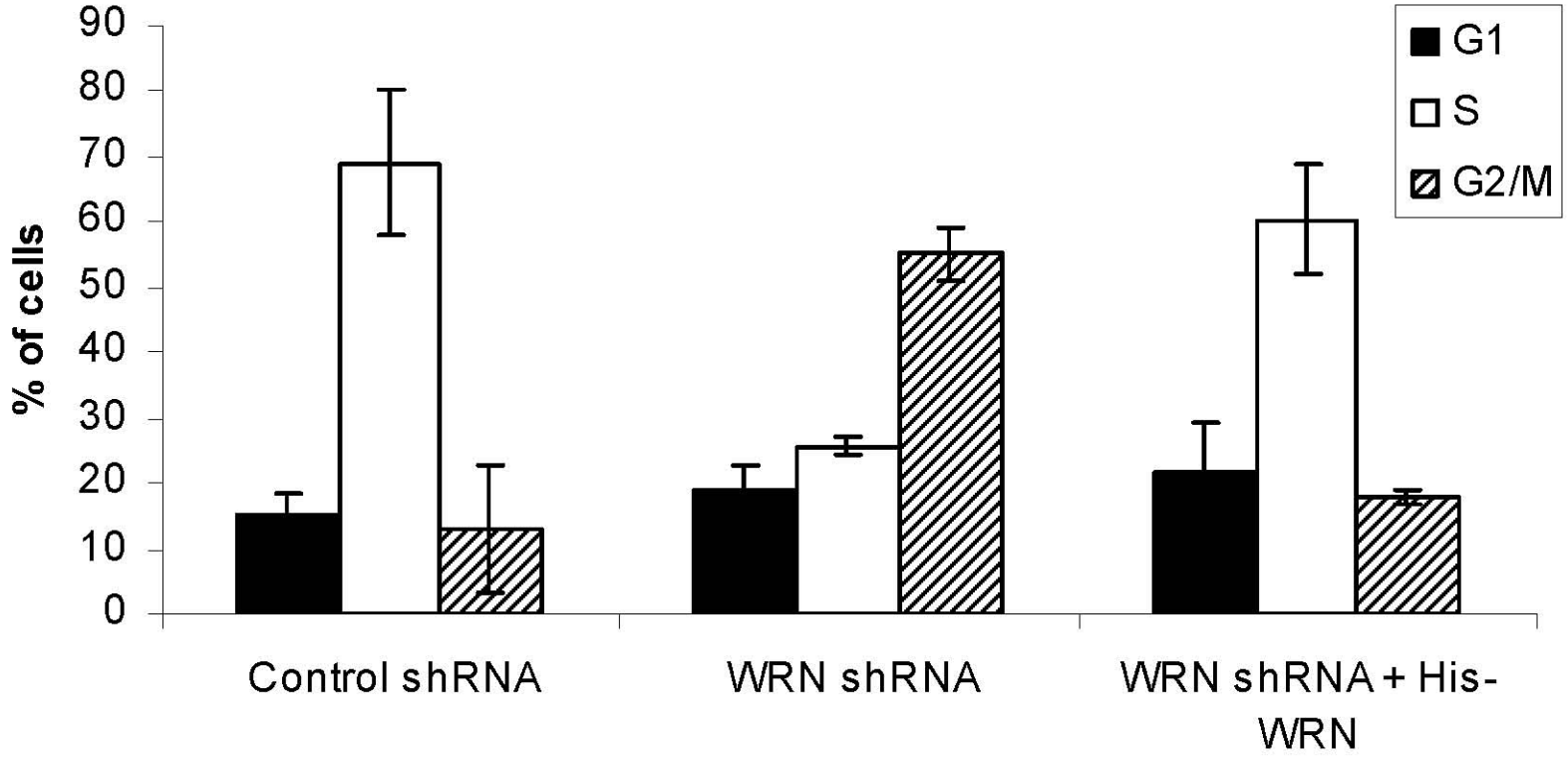

Control shRAN cells, WRN shRNA cells, and the WRN shRNA cells complemented with His-WRN using Polyfect reagent (Qiagen) were treated with PUVA (0.1 μg/ml) , and cells were collected 24 h post-treatment for flow cytometric analysis.

Cheng et al. Supplemental Fig S4

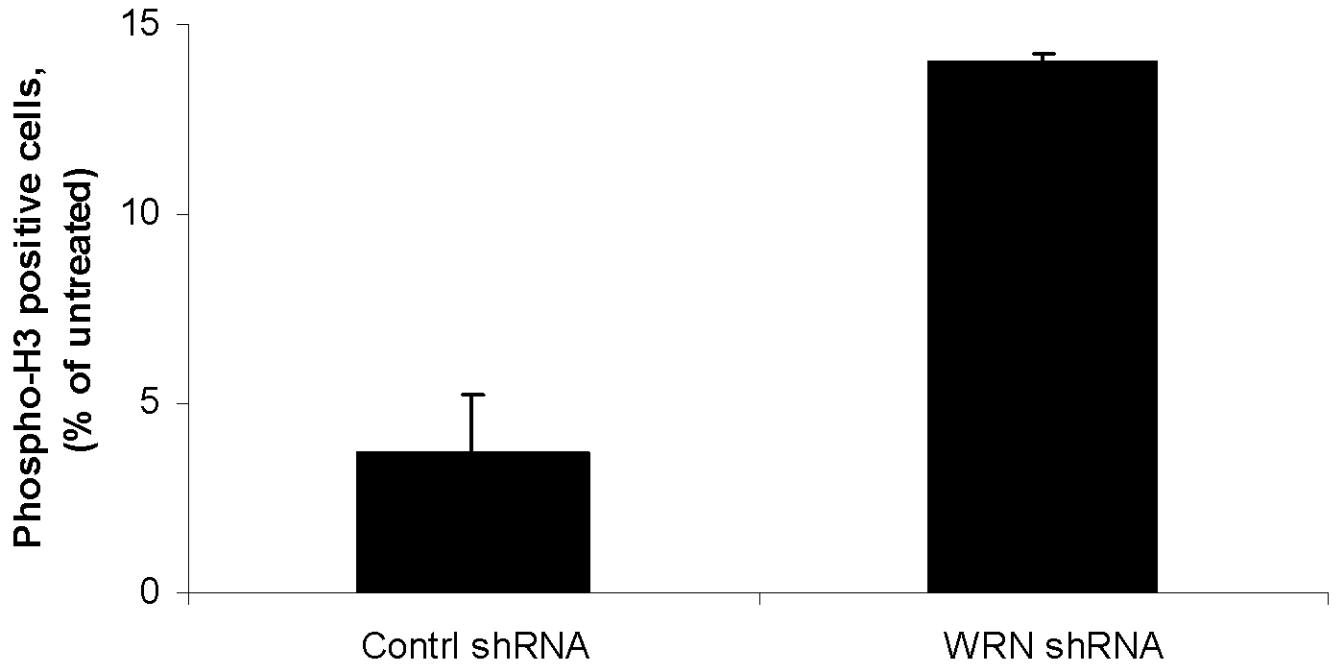

WRN shRNA cells show increased mitotic entry after PUVA treatment.
Control and WRN shRNA U-2 OS cells were treated with PUVA (0.1 μg 8-methoxypsoralen/ml) and harvested after 12 h. The relative fraction of phospho-H3 positive cells was determined by flow cytometry. Values are expressed as a percentage of the unirradiated control (n = 3).

Cheng et al. Supplemental Fig S5

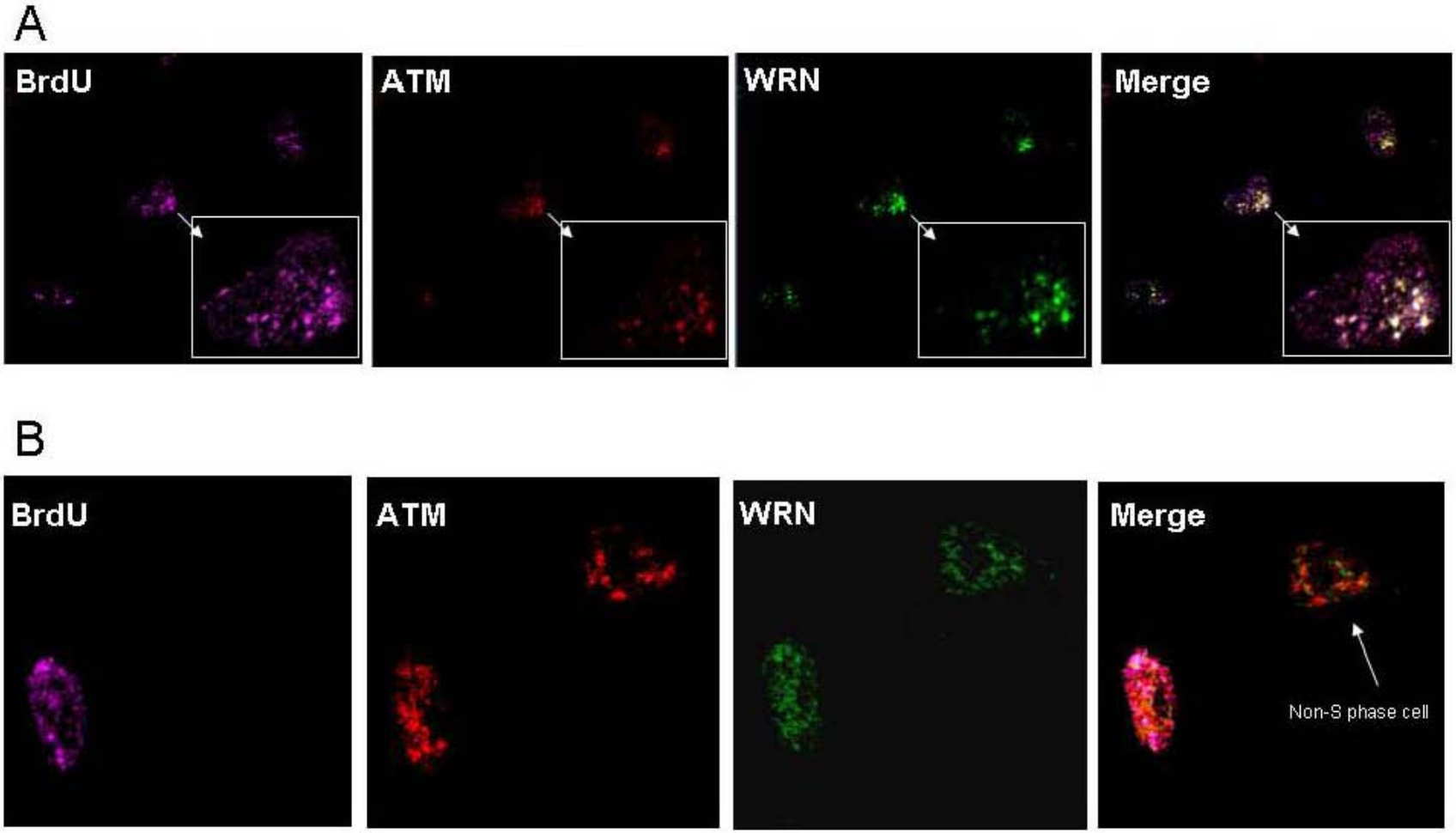

ATM co-localizes with WRN at sites of DNA replication.

U-2 OS cells were pulse-labeled with BrdU for 0.5 h, fixed, and stained with rabbit antibodies against ATM (red), mouse antibodies against WRN (green), and sheep antibodies against BrdU (purple).
(A) shows unperturbed S phase and (B) shows non-S phase cells.

Cheng et al. Supplemental Fig S6

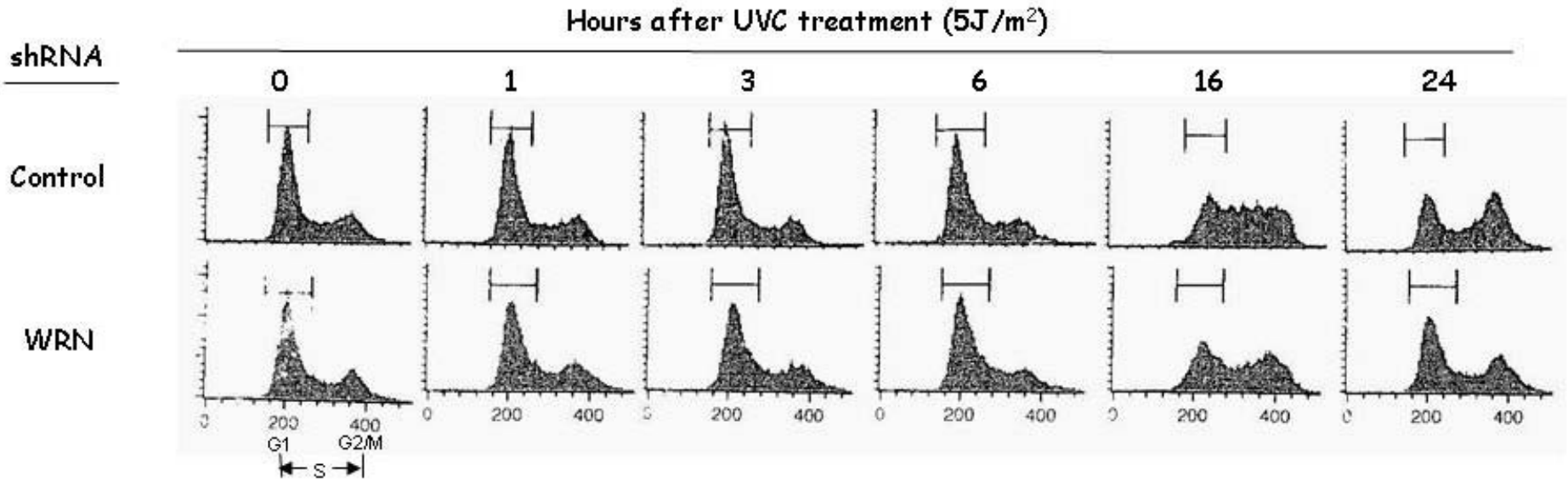

Cell cycle profiles in control and WRN shRNA U-2 OS cells treated with UV.
Cells were treated with UVC (5J/m^2, at a rate of 1J/sec). Cells were harvested at the indicated time points and Analyzed by flow cytometry as described in Materials and Methods.

Cheng et al. Supplemental Fig S7